ACS Sustainable Chemistry & Engineering

Research Article

pubs.acs.org/journal/ascecg

Preparation of Cellulose/Graphene Composite and Its Applications for Triazine Pesticides Adsorption from Water

Che Zhang,[†] Run Z. Zhang,[†] Yong Q. Ma,*[,†] Wen B. Guan,[†] Xiao L. Wu,[†] Xue Liu,[†] Hong Li,[†] Yan L. Du,*[,‡] and Can P. Pan[†]

[†]College of Science, China Agricultural University, Beijing 100193, China

[‡]Plant Science and Technology College, Beijing University of Agriculture, Beijing 102206, China

Supporting Information

ABSTRACT: This study prepares a new form of cellulose/graphene composite (CGC) by mixing dissolved cellulose with graphene oxide and reducing it with hydrazine hydrate. The composite particles achieve higher adsorption levels than five other sorbents (graphite carbons, primary secondary amine (PSA), graphite carbon black (GCB), cellulose, and graphene) for six triazine pesticides. The adsorption process only requires adding 30 mg of CGC for 10 mL of solution of triazine pesticides. The mixture is hand-shaken five times at pH 9. The equilibrium adsorption isotherm reveals that the Langmuir model describes the adsorption process better. Thermodynamic parameters indicate that adsorption is spontaneous, favorable, and endothermic in nature. Furthermore, the CGC is very stable and can easily be recycled using a simple organic solvent. The adsorption efficiency of the CGC is still over 85% after six times of recycling.

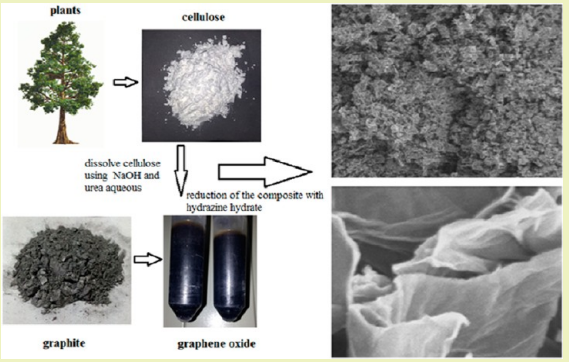

KEYWORDS: *Triazine pesticides, Cellulose, Graphene, Adsorbent, Thermodynamics*

INTRODUCTION

Triazine pesticides have been widely used in recent years to control weed in several crops. These pesticides play a crucial role in the cultivation of cereals, such as maize and rice.[1] Their residues have, however, become a major source of environmental contamination. Triazine pesticides also cause potential hazard for human beings, which include cancers, birth defects, and interruption of hormone functions.[2] In 2006, ametryn, atrazine, prometryn, and simazine were listed in the national and European Union-coordinated monitoring program for routine monitoring and consumer risk assessment.[3]

Conventional methods of removing triazine pesticide residues in water are still widely used. These techniques have low efficiency and comprise particle coagulation−flocculation, sedimentation, and dual media filtration.[4−7] The more advanced final treatment steps, which usually involve oxidation by H_2O_2 or O_3 and granular-activated carbon (GAC) filtration, are generally considered to be effective,[8] although the carbon filters are rapidly saturated and their efficiency to eliminate pesticides decreases with the high presence of natural organic matter caused by competitive adsorption.[9] Toxic chemical byproducts may also develop in the GAC filters under some conditions.[10,11] Therefore, developing an efficient sorbent with a simpler separation process will be a significant achievement.

Cellulose is the most abundant natural polymer in nature. This polymer is renewable, biodegradable, and biocompatible. Using cellulose is conducive to sustainable development and long-term economic interests.[12] However, cellulose is not easily dissolved in common solvents nor is it impossible to melt because of its strong inter- and intramolecular hydrogen bonds and high degrees of polymerization and crystallinity.[13] Many scientists have used specific solvents to disrupt hydrogen bonds and dissolve cellulose.[14] Shi et al.[15] used 7 wt % NaOH and 12 wt % urea aqueous solution with cooling to dissolve the cellulose rapidly. According to this important discovery, blending other materials with the cellulose in a solvent is an efficient approach to modify cellulose.

Meanwhile, graphene continues to play an important role in many fields such as carbon nanomaterials because of its unique optical, electrical, mechanical, and structural properties.[16] The large delocalized p-electron system and high theoretical specific surface area of graphene make the material suitable for adsorption of heavy metals, organic dyes, and pesticide residues.[17] The 2D flat structure of graphene is also effective in improving the mechanical and thermal properties of composite materials. Feng et al.[18] used a cellulose/graphene nanocomposite as a mechanically strong, flexible, and conductive film. Weng et al.[19] utilized graphene−cellulose for paper flexible supercapacitors. However, only a few researchers have noticed the adsorption properties of graphene. Shi et al.[20]

Received: August 12, 2014
Revised: December 14, 2014
Published: January 30, 2015

DOI: 10.1021/sc500738k
ACS Sustainable Chem. Eng. 2015, 3, 396−405

studied methylene blue adsorption using a magnetic cellulose/graphene oxide (GO) composite. The composite provides an efficient, stable, and environmentally friendly adsorbent for practical application in the treatment of dye wastewater. Shi et al. used GO in a composite, which contained many oxygen groups and played a major role in the adsorption process. On the contrary, the present research aims to explore mainly the potential adsorption capability of cellulose. Hence, a reduced graphene oxide (RGO) rather than a GO is used.

After several attempts, we successfully obtained a cellulose/graphene composite (CGC) by a new method. By using hydrazine hydrate at a certain temperature, graphene oxide can be reduced slowly. At the same time, dissolved cellulose is added in solution slowly. After that, cellulose became the main skeleton in the composite according to the characterization. This new sorbent was compared with graphite carbons, PSA, GCB, cellulose, graphene. The results show that the CGC effectively adsorbs six different triazine pesticides (structures listed in Figure 1).

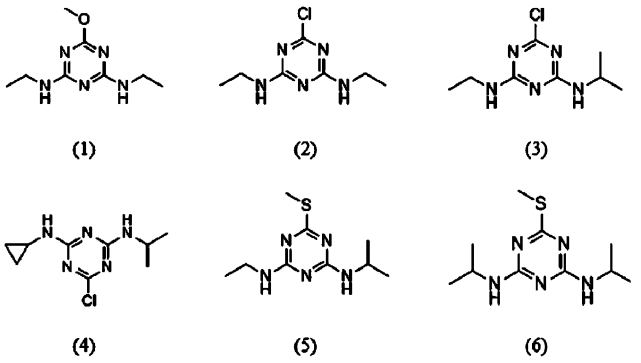

Figure 1. Structures of six triazine pesticides: (1) simeton, (2) simazine, (3) atrazine, (4) cyprazine, (5) ametryn, and (6) prometryn.

EXPERIMENTAL SECTION

Reagents and Materials. Simeton, simazine, atrazine, cyprazine, ametryn, and prometryn were obtained from J&K Scientific, Ltd. Chromatographic grade acetonitrile and ethyl acetate in glass containers were purchased from MREDA Co., Ltd. (Beijing, China). Expandable graphite was obtained from Qingdao Hensen Graphite Co., Ltd. (Qingdao, China). Microcrystalline cellulose was purchased from Sinopharm Chemical Reagent Beijing CO., Ltd. Ultrapure water was obtained from a Milli-Q water purification system (Millipore, Billerica, MA, U.S.A.). All other reagents employed were analytically pure as purchased from Sinopharm Chemical Reagent Beijing CO., Ltd.

Preparation of Graphene Oxide. Graphene oxide was prepared according to Hummers's method.[21] There may be some change in the synthesis steps; the specific method refers to our previous literature.[17]

Preparation of CGC. First, 7 wt % (14 g) NaOH, 12 wt % (24 g) urea, and 81 wt % (162 g) water were mixed together. The aqueous solution was precooled to −12 °C in an ice−salt bath. Cellulose (2 g) was immediately dispersed into the mixed aqueous solution after stirring for 30 min at ambient temperature and centrifuged for 5 min to obtain a transparent cellulose solution. Cellulose solution and graphene oxide (80 mL, 10 mg/mL) were added to a three-necked flask with an ultrasonic treatment. Then, 85% hydrazine hydrate (120 mL) was added to the solution, and the mixture was heated to 80 °C in an oil bath for 12 h. Next, the suspension was washed with distilled water until pH 7. The mixture is frozen at −20 °C in the fridge overnight. Finally, the frozen samples were freeze-dried in a lyophilizer at −50 °C and 0.0014 mbar vacuum for 3 days.

Adsorption Tests on CGC. To test the effect of time on adsorption, 30 mg of CGC was added into the freshly prepared solution of six triazine pesticides (10 mL, 1 mg/L). The sample was stirred on a vortex mixer for 0 (shaken five times by hand), 1, 3, and 5 min. Different dosages of the CGC (10−80 mg) were investigated to get the proper doses for removing the six triazine pesticides, and different pH values (3−11) were also examined. For the adsorption isotherm experiments, 30 mg of GCS was added into prometryn solution (10 mL) with a concentration ranging from 0.3 to 15 mg/L and shaking by hand five times to reach equilibrium. In order to study the temperature of the adsorption process of the CGC, experiments were conducted at 298, 308 and 318 K, respectively.

Triazine Pesticides Determination. After the adsorption process, the solution was centrifuged for 5 min at 3800 rpm. The supernatant was discarded. Acetonitrile as desorption solvent (10 mL) and NaCl (1 g) were added, and the mixture was vortexed for 30 s to desorb the analytes. Then the mixture was centrifuged at 3800 r/min for 5 min. Five milliliters of the supernatant was transferred to a flask and concentrated nearly to dryness on a rotary evaporator at 40 °C. Finally, the mixture was dissolved in 2 mL of ethyl acetate. The analysis of triazine pesticides was performed by an Agilent 6890N GC-5975B MSD (Agilent Technologies, Palo Alto, CA, U.S.A.). The separation was achieved on a fused silica capillary column (HP-5 MS, 30 m × 0.25 mm i.d., with 0.25 mm film thickness). The column temperature was programmed at 120 °C for 1 min initially. Then the temperature increased to 175 °C at a rate of 35 °C/min and held for 1 min, then increased to 215 °C at a rate of 4 °C/min and held for 1 min, and finally increased to 260 °C at a rate of 30 °C/min and held for 5 min. The ion source, quadrupole, and transfer line temperatures were 230, 150, and 280 °C.

Characterization. Several analytical methods were used to confirm the deposition of the CGC. Fourier transform infrared (FTIR) spectroscopy was recorded on a PerkinElmer 2000 in the range of 400−4000 cm^{-1}. X-ray photoelectron spectroscopy (XPS, ESCALAB 250Xi) and a BrukerD/MAX 2400 X-ray diffractometer(XRD) were both used for structure analysis. Raman spectroscopy was carried out on a LabRAM HR Evolution. The surface morphologies of the CGC samples were examined by scanning electron microscopy (SEM) on a Hitachi S-4800. TEM images of the prepared GO and RGO were recorded over a JEOL JEM-2011 operated at 100 kV. The elemental analyses were carried out by using a Thermo Flash EA-1112 series analyzer.

RESULTS AND DISCUSSION

Characterization Analysis. *FT-IR Analysis.* The FT-IR spectra of reduced graphene oxide, CGC, and cellulose are shown in Figure 2; the peak at 1605 cm^{-1} (Figure 2a) corresponds to C═C stretching vibrations of the unoxidized graphitic domains.[22] The cellulose (Figure 2c) shows O−H stretching (3200−3500 cm^{-1}) and C−H stretching (2850−3000 cm^{-1}) corresponding to the aliphatic moieties. The strong absorption peak at 1058 cm^{-1} should be the stretching vibration of the C−O−C bond in cellulose.[23] As shown in the CGC (Figure 2b), one characteristic absorbance band located at 2917 cm^{-1} corresponds to the stretching vibrations of the C−H, which are methyl, methylene, and methane of the cellulose.[20] The peak at 1058 cm^{-1} indicates there is a C−O bond of cellulose. In addition, the peak at 1608 cm^{-1} corresponds to the C═C stretching vibrations of reduced graphene oxide.[24] These characteristic peaks show that reduced graphene oxide and cellulose were both introduced into the CGC composites.

X-ray Diffraction (XRD) Analysis. Figure 3 presents the XRD patterns of cellulose, cellulose/graphene composite (CGC), and RGO. For the CGC, a sharp peak at 2θ = 8.10° is ascribed to the (001) plane of GO. The broad diffraction peak centered at 2θ = 23.80° is also observed in the XRD

DOI: 10.1021/sc500738k
ACS Sustainable Chem. Eng. 2015, 3, 396−405

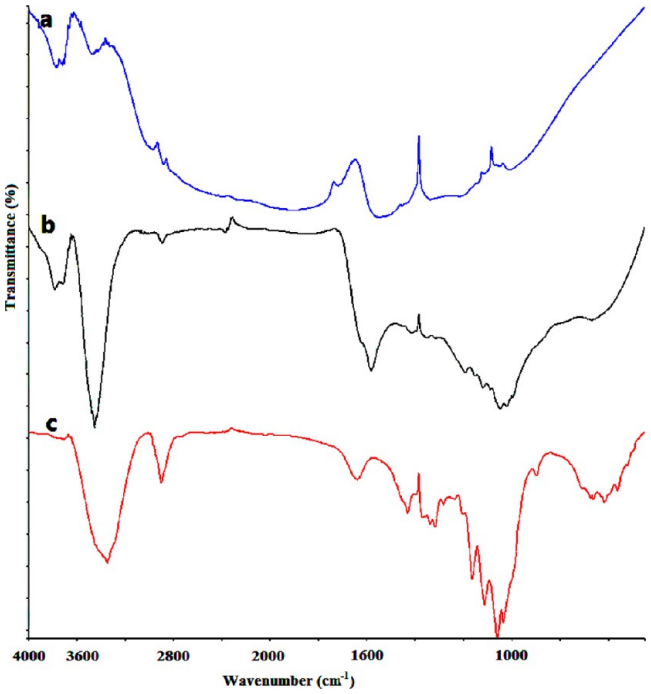

Figure 2. FT-IR spectra of (a) RGO, (b) CGC, and (c) cellulose.

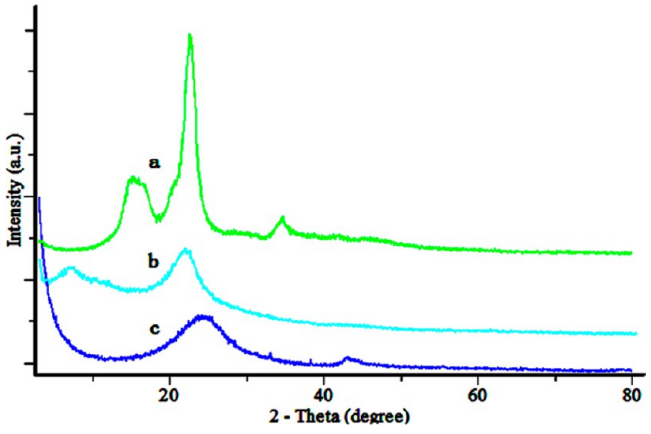

Figure 3. X-ray diffraction patterns for (a) cellulose, (b) CGC, and (c) RGO.

pattern of the RGO, which implies the existence of the RGO in the CGC.[25] The microcrystalline cellulose exhibits two main peaks at 2θ = 14.86° and 22.74°, which correspond to the (110) and (200) planes, respectively.[26] The broad diffraction peaks suggest that the CGC particles and the cellulose both have an amorphous nature.[27]

Raman Analysis. Raman spectroscopy is an effective structural testing instrument for nanomaterials. Figure 4 illustrates the Raman patterns of the GO, CGC, and RGO. Accordingly, D and G peaks around 1352 and 1598 cm^{-1}, respectively, are observed for the CGC sample. This observation confirms the presence of RGO.[28,29] The ID/IG ratio of the GO is close to 0.88, whereas that of the CGC is 1.17. The reaction from GO to CGC by hydrazine hydrate results in a higher ID/IG ratio because of a decrease in the sp^2 cluster size caused by removing oxygen groups.[17,30]

XPS Analysis. Figure 5 shows XPS survey scan spectra of the CGC and CGC containing 72.0% C and 25.2% O; its O/C atomic ratio is 0.35. XPS data of GO and RGO are given in

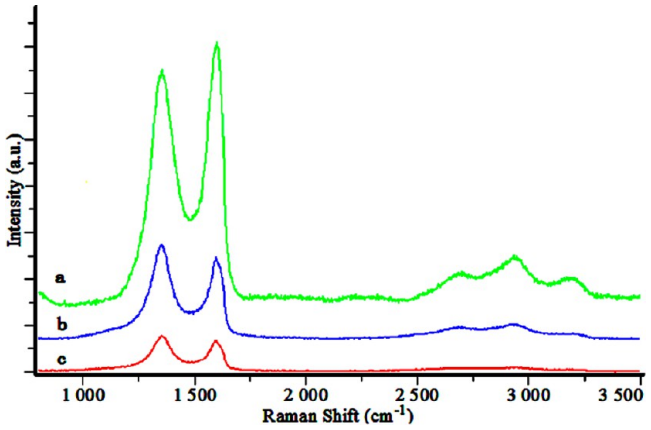

Figure 4. Raman spectra of (a) GO, (b) CGC, and (c) RGO.

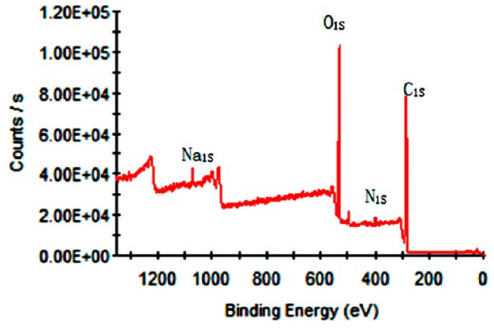

Figure 5. XPS survey scan spectra of CGC.

Figure S5 of the Supporting Information. GO contains 64.9% C and 34.4% O, and its O/C atomic ratio is 0.53. Microcrystalline cellulose ($(C_6H_{10}O_5)_n$) contains 44.4% C and 49.4% O, and its O/C atomic ratio is 1.11 theoretically. In contrast to GO, the intensity of the oxygenated functional groups of RGO become weaker (Figure S5(b), Supporting Information), which indicates the reduction of GO with hydrazine hydrate. The reduction from GO to RGO is incomplete, and the O/C atomic ratio of the RGO is about 0.12. This evidence suggests that the oxygen-containing groups of cellulose exists widely in the CGC.[31] The CGC contained a small amount of N and Na, which was observed at 400 eV in the N_{1s} spectrum and 1071 eV in the Na_{1s} spectrum, respectively. This could explained that urea and NaOH are used in dissolving cellulose.

SEM Analysis. The scanning electron microscopy (SEM) images of the CGC in Figure 6 exhibit a clear rough surface and homogeneous 3D porous structures, whereas the cellulose has a smooth and homogeneous surface morphology according to previous reports.[32] The surface becomes rough and contains a lamellar structure when the RGO is introduced.[33] The CGC shows many porous structures beneath the sample surfaces, which might be caused by the supporting effect of the RGO sheets during coagulation.[34,35] As active adsorption sites, these rough and wrinkled structures in the CGC provide an advantageous condition for attracting triazine pesticides and remarkably improve the adsorption rate and capacities.[20]

TEM Analysis. Figure 7A and B, respectively, illustrates a high-resolution transmission electron microscopy (TEM) image of the RGO and a low-magnification TEM image of the GO. The former shows a few-layer graphene membrane near its edge. The number of dark lines indicates the thickness of two to four layers.[36] The ordered graphite lattices are visible

DOI: 10.1021/sc500738k
ACS Sustainable Chem. Eng. 2015, 3, 396−405

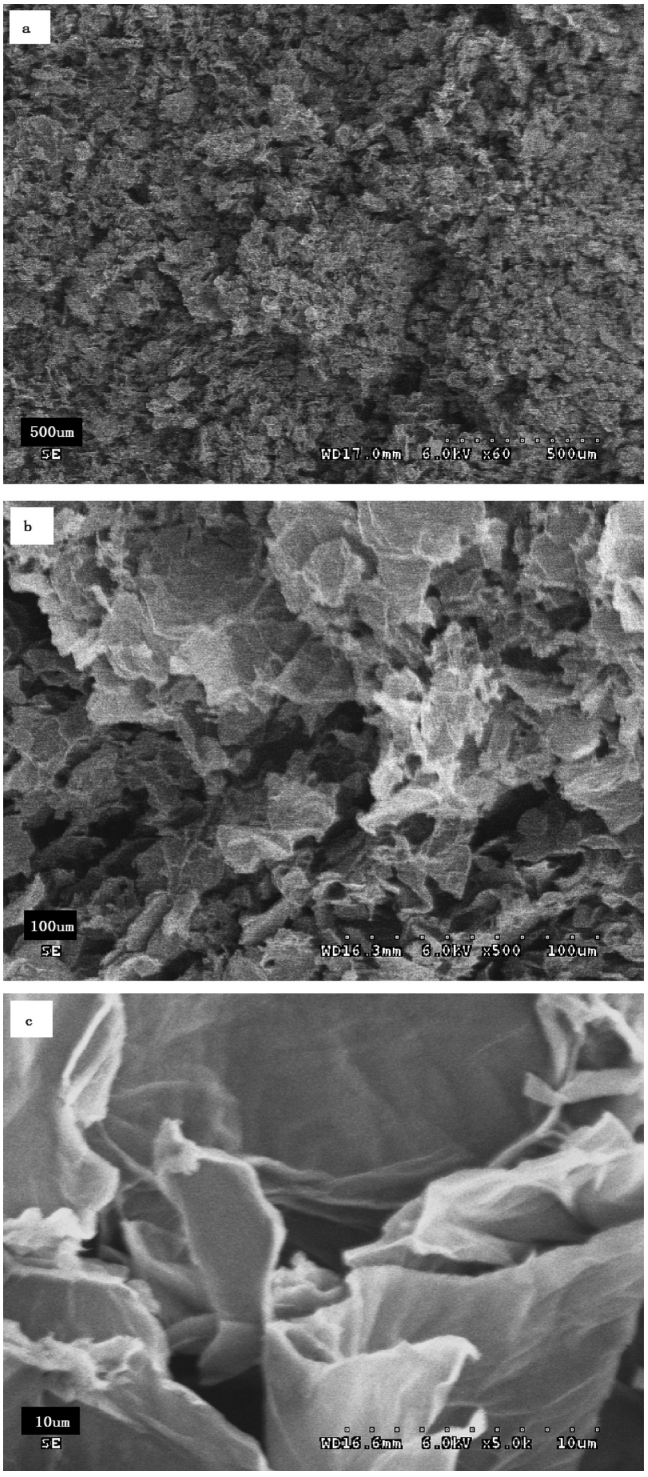

Figure 6. SEM images of the different morphologies of CGC sheets: (a) scale = 500um, (b) scale = 100um, and (c) scale = 10um.

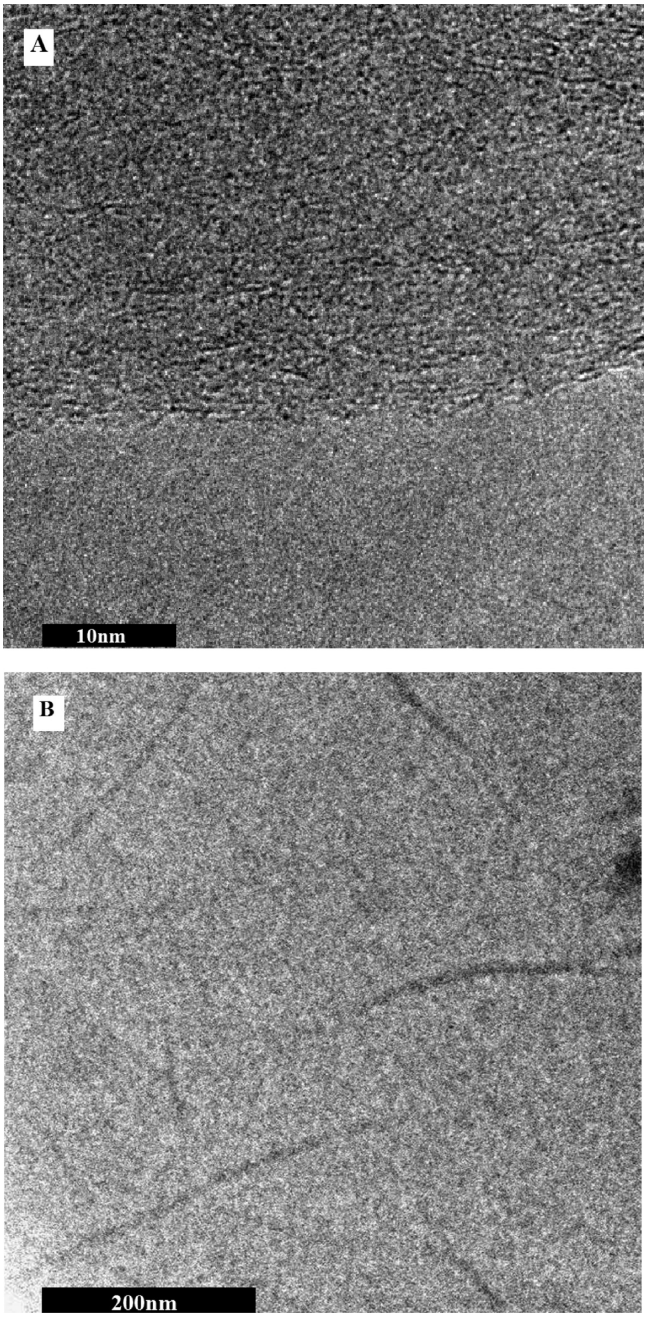

Figure 7. (A) TEM images of a few-layer graphene membrane near its edge. (B) TEM image of graphene oxide nanosheets.

and the disordered regions are found, which indicate that graphene is partially restored to the ordered crystal structure after the reduction reaction with hydrazine hydrate.[37] The TEM image of the GO illustrates the amorphous and disordered structure of the GO nanosheet. These nanosheets tend to congregate together to form multilayer agglomerates. This result is consistent with that of previous reports.[38]

Elemental Analysis. The elemental analysis is performed using a Thermo Flash EA-1112 series analyzer. The analysis data for the composite show that the CGC contains 1.84% N, 52.28% C, and 3.63% H. This result reveals a high oxygen content (42.25%), which suggests that oxygen-containing groups of cellulose widely exist in the CGC. The trace element of N produces the urea used in dissolving cellulose. The elemental composition of the microcrystalline cellulose ($(C_6H_{10}O_5)_n$) is computable (i.e., C, 44.4%; O, 49.4%). These results demonstrate that a high content of oxygen-containing functional groups of cellulose is introduced into the CGC.

Optimization of CGC Composite Preparation. The effect of two components of the CGC was investigated with a single-factor method. The experimental results are shown in Figure 8. With an increasing dosage of cellulose or graphene oxide, the

DOI: 10.1021/sc500738k
ACS Sustainable Chem. Eng. 2015, 3, 396−405

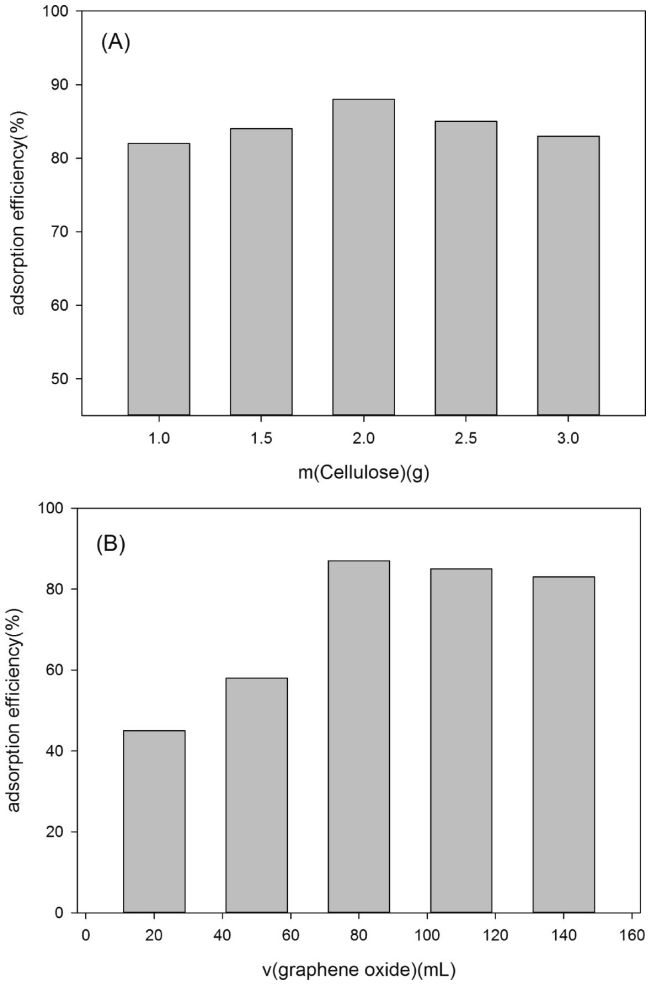

Figure 8. Effects of different qualities of each component on the adsorption efficiency: (A) v(graphene oxide) = 80 mL and (B) m(cellulose) = 2.0 g.

average adsorption efficiency of the CGC for six triazine pesticides was increased first and then decreased. The optimal values (mass of cellulose, 2 g; mass of GO, 80 mL, 10 mg/mL) of the variables can be obtained.

Adsorption Tests. In adsorption tests, the adsorption time, CGC dose, and pH of the solution were optimized to achieve maximum adsorption efficiency.

Effects of Time on Adsorptive Capacity of CGC. The duration and method of mixing were key factors affecting the adsorption efficiency. In this test, 30 mg of CGC was added to the solution and mixed by vortexing for different durations (0, 0.5, 3, 5, 10 min) before the solutions were tested. The data in Figure 9A make it clear that no stirring (0 min, the solution was just shaken five times by hand) produced the most efficient adsorption, and it is more convenient than trying to use a vortexer. It might be explained that a large number of vacant surface sites were available for adsorption during the initial stage. However, with a lapse of adsorption time, the surface may be affected by vortexing. Therefore, shaking five times by hand was chosen as the standard treatment in this experiment.

Effects of Dosage on Adsorptive Capacity of CGC. The dose of adsorbent plays a crucial role in adsorption efficiency. Different CGC doses in the range of 5−100 mg (5, 10, 20, 30, 50, 70, 100 mg) were added to 10 mL solutions containing 1 mg/L of each of the six triazine pesticides. The results are shown in Figure 9B. It shows that the efficiency increased with increasing adsorbent dosage because more surface area was available for adsorption. However, the data of 30 mg shows equally good adsorption performance as 50 mg and 70 mg. For the reason for economic concerns, 30 mg of adsorbent was chosen as the standard treatment in this experiment.

Effects of pH on Adsorptive Capacity of CGC. For water samples, pH is a key factor affecting the ionic states of the target analytes and may therefore influence the adsorption properties of the CGC.[39] The pH of the solution was adjusted to 1, 3, 5, 7, 9, and 11 with HCl or NaOH. The data in Figure 9C shows that with increasing pH adsorptive capacity of the CGC increased and reached the maximum with pH 9 except for cyprazine (pH 11). Then, the pH of the solution was adjusted to 9 in the following tests.

Comparison of RGO and GO in Cellulose Composite Regarding Adsorption. The importance of the RGO in the CGC is supplemented with pertinent experimental data presented in Figure 10. The method of preparing the GO−cellulose composite is identical to that of the CGC, albeit without the chemical reduction step. The RGO−cellulose composite obviously has a better adsorption capacity than the GO−cellulose composite. Recent studies have shown many differences in the adsorption capacities of the RGO and GO for different pesticides.[40] Efficient GO adsorption basically depends on charge-based interactions between the GO and the adsorbates. However, the RGO performs better for the six triazine pesticides in this study, which indicates that the interactions between the CGC and the triazine pesticides are possibly electrostatic and van der Waals-type interactions. Moreover, the GO−cellulose composite is difficult to separate from the treated water because of the loose combination of the GO and the cellulose, which may hinder its adsorption capacity, regeneration, and reuse. For the CGC, however, the RGO and the cellulose are both introduced into the CGC composites after chemical reduction with the help of hydrazine hydrate. This close combination enhances the adsorption capacity and is more conducive to CGC regeneration and reuse.

Consistency of Adsorption Properties and Comparison with Five Other Sorbents. The following optimal conditions are chosen to test the repeatability of the results: 30 mg of CGC is added to the solution of the six triazine pesticides. The solution pH is adjusted to 9 with NaOH, and the mixture is hand-shaken five times. This test is repeated five times under optimal conditions. The relative standard deviations are all under 5.0% (Table 1), which confirm the efficiency, accuracy, and reliability of the tests. Six sorbents (i.e., CGC, graphite carbons, microcrystalline cellulose, PSA, GCB, and graphene) are tested under the optimal conditions and compared in terms of their abilities to adsorb from a 10 mL solution of triazine pesticides with 1 mg/L starting concentration. Figure 11 presents the results, where the adsorptive capacities of the cellulose and the PSA are unsatisfactory. The CGC generally has a better adsorption capacity than the other five sorbents. However, its adsorption capacity does not perform very well at prometryn compared with that of the GCB or the graphene. It should be noted, however, that the GCB is too expensive to use widely. Meanwhile, the performance of graphene is very poor with simeton and simazine. As observed in the elemental and X-ray photoelectron spectroscopy (XPS) analyses, the CGC containing a low graphene percentage obtains a better adsorption capacity for these six triazine pesticides with the help of the cellulose. Overall, the CGC can be regarded as a

DOI: 10.1021/sc500738k
ACS Sustainable Chem. Eng. 2015, 3, 396−405

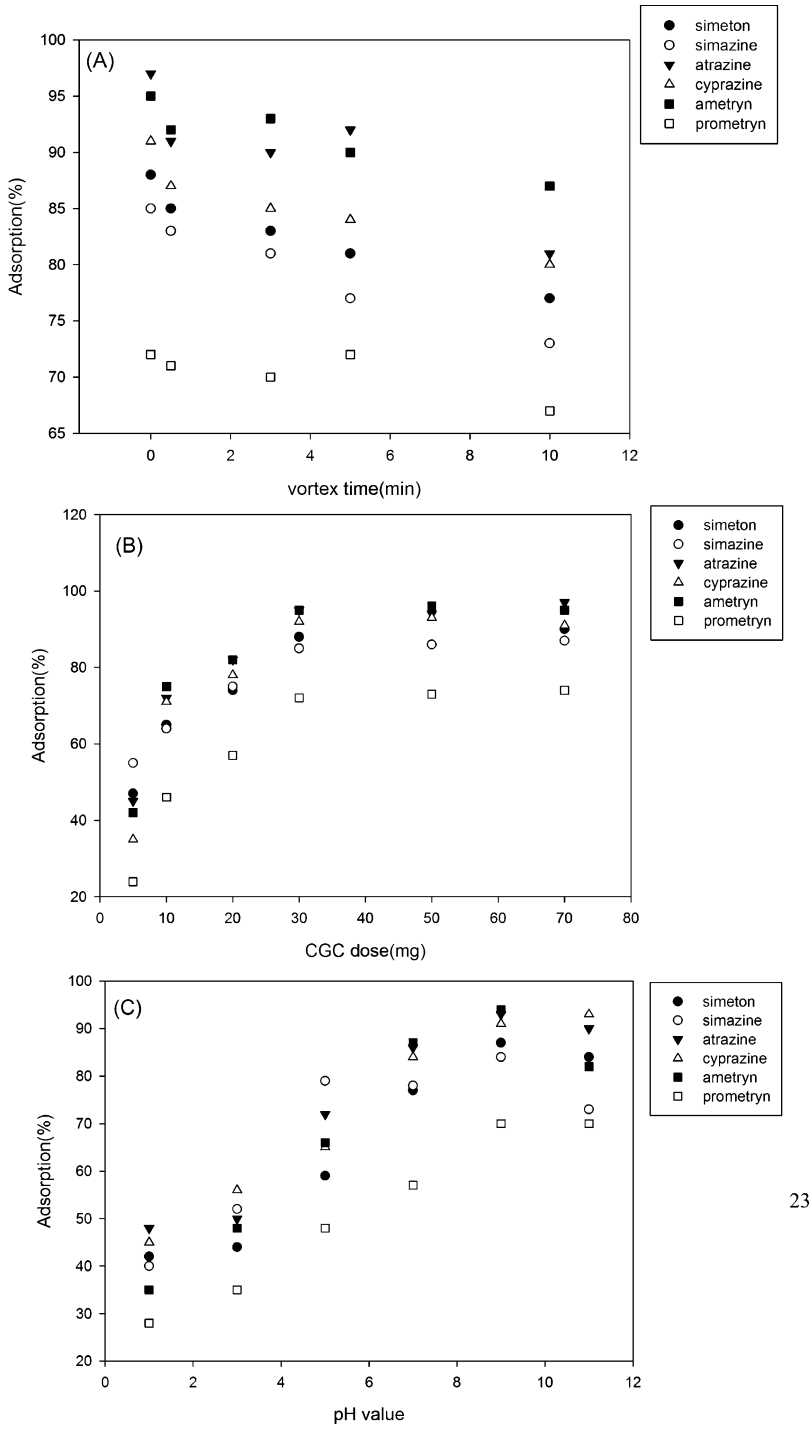

Figure 9. (A) Effects of the vortex time on the adsorption. (B) Effect of the CGC dose on the adsorption. (C) Effect of pH on the adsorption.

suitable sorbent for treating these six triazine pesticides in water considering its efficient adsorption performance and low-cost practical application.

Adsorption Mechanism of CGC for Six Triazine Pesticides. Understanding how the adsorbates interact with the particles is crucial in exploiting the differences among the six triazine pesticides adsorbed by the CGC. The strong π-bonding network in the triazine pesticides and the electron-donating abilities of the N, S, and O atoms can generally assist adsorption.[17,41] These six triazine pesticides have a similar structural formula and exactly the same N atoms (Figure 1). Hence, the π-bonding networks of all the pesticides are almost identical. Therefore, the S, O, and Cl atoms and the van der Waals-type interactions may be the main causes of the differences.[40,42,43] First, the structures of atrazine, ametryn, and prometryn are compared. Atrazine has an O atom, while the others have S atoms. Ametryn, which contains an S atom, is more able to donate electrons. Its adsorption efficiency is also better than that of atrazine. Prometryn, which performs worst among the six triazine pesticides, has an additional branched structure that weakens the van der Waals-type interactions. This branched structure is not conducive to the interactions between the CGC and prometryn. Second, simazine, atrazine, and cyprazine contain an electron-withdrawing nature of

23

DOI: 10.1021/sc500738k
ACS Sustainable Chem. Eng. 2015, 3, 396−405

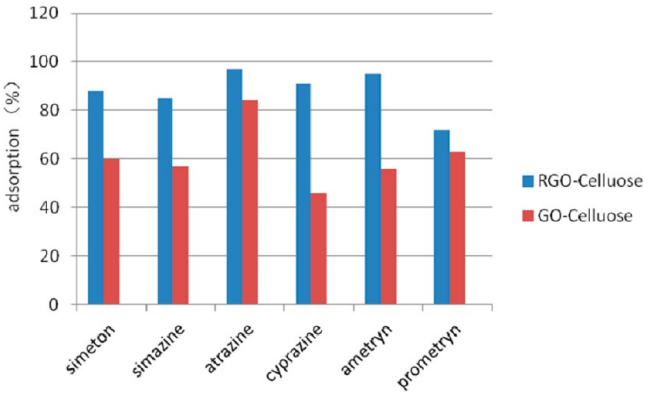

Figure 10. Comparison of RGO and GO in cellulose composite with adsorption.

Table 1. Consistency of Absorption Performance (%) of CGC

pesticide	RSD[a] [%]
simeton	1.7
simazine	3
atrazine	2.1
cyprazine	4.1
ametryn	2.9
prometryn	3.4

[a]Relative standard deviation, $n = 5$.

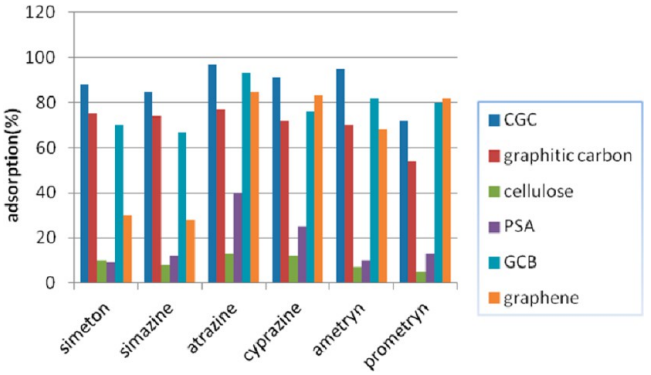

Figure 11. Comparison of the adsorption capacity of CGC, graphitic carbon, cellulose, PSA, GCB and graphene toward six triazine pesticides.

chlorine atoms. Chlorine atoms could lead to an acidic π system, which readily forms complexation with the π system with no derivative and benefits the adsorption process.[44]

Adsorption Isotherms. Tests on adsorption isotherms are helpful for us understanding the process and principle of adsorption systems. In this paper, ametryn was selected and tested to get the adsorption isotherms. Figure 12 shows the adsorption isotherms of ametryn on CGC over the concentration from 1 to 15 mg/L at 298, 313, and 323 K. The experimental data are modeled with the Langmuir and Freundlich models (Tables 2 and 3.

The uptake of ametryn at equilibrium, q_e (mg/g), was calculated by the following equation

$$q_e = \frac{(C_0 - C_e)V}{m} \quad (1)$$

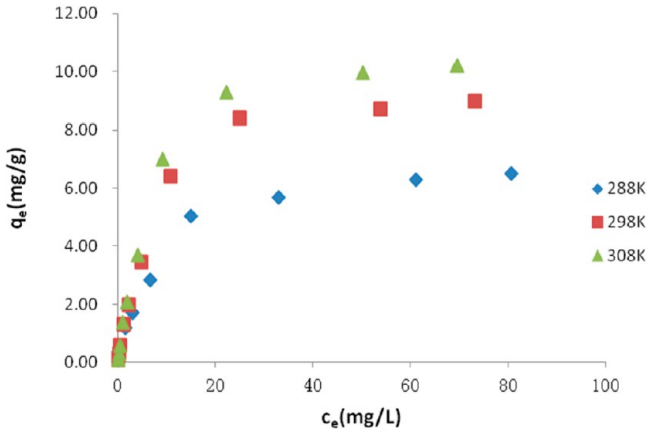

Figure 12. Adsorption isotherms of ametryn on CGC.

Table 2. Parameters of Langmuir Isothermal Adsorption Equations of CGC to Ametryn

T (K)	regression equation	q_m	K_L	R^2
288	$1/q_e = 0.7460/C_e + 0.1549$	6.4558	0.2076	0.9801
298	$1/q_e = 0.5064/C_e + 0.1172$	8.5324	0.2314	0.9843
308	$1/q_e = 0.4148/C_e + 0.1043$	9.5877	0.2514	0.9833

Table 3. Freundlich Isothermal Adsorption Equations of CGC to Ametryn

T (K)	regression equation	n	K_F	R^2
288	$\ln q_e = 0.6101 \ln C_e - 0.3682$	1.6391	0.6919	0.9635
298	$\ln q_e = 0.6371 \ln C_e - 0.0341$	1.5696	0.9665	0.9654
308	$\ln q_e = 0.6419 \ln C_e + 0.1239$	1.5579	1.1319	0.9651

where C_0 represents the initial concentration of the solution (mg/L), V represents the volume of the solution, and m represents the adsorbent dose (g).

The linear forms of Langmuir equation and Freundlich equation can be written as

$$\text{Langmuir isotherm: } \frac{C_e}{q_e} = \frac{1}{q_m K_L} + \frac{C_e}{q_m} \quad (2)$$

$$\text{Freundlich isotherm: } \ln q_e = \ln K_F + \frac{\ln C_e}{n} \quad (3)$$

where K_L (L/mg) is the Langmuir equilibrium constant, q_m is the maximum adsorption capacity (mg/g), and K_F ((mg g^{-1})(L mg^{-1})$^{1/n}$) and n are Freundlich constants that related to the adsorption capacity and adsorption intensity.

All of the linear correlation coefficients R^2 of the Langmuir isotherm are larger than 0.98, indicating that adsorption of ametryn conforms to the Langmuir adsorption model, which means the adsorption process of ametryn is consistent with the assumption of the Langmuir model that the adsorbate that has been adsorbed on the surface of the solid adsorbent would cease to migrate (Table 2). The reason can be explained that the functional groups (carboxyl, hydroxyl, and epoxy functional groups), as adsorption sites almost distribute on the outer surface of the CGC.[20] In addition, the adsorption process is homogeneous and monolayer.[45]

Besides, the maximum adsorption capacities and K_L for ametryn on the CGC increased with increasing temperature, indicating that higher temperature is more conductive to the adsorption process.

DOI: 10.1021/sc500738k
ACS Sustainable Chem. Eng. 2015, 3, 396−405

Effect of Temperature on Adsorption. For the purpose of studying the temperature of the adsorption process of ametryn, experiments were conducted at 298, 308, and 318 K, respectively. The thermodynamic parameters can be calculated by the van't Hoff equation.[46]

$$\ln\left(\frac{Q_e}{C_e}\right) = -\frac{\Delta H}{RT} + \frac{\Delta S}{R} \quad (4)$$

Gibbs free energy can be calculated from the following relation

$$\Delta G = \Delta H - T\Delta S \quad (5)$$

where T is absolute temperature in Kelvin (K), and R is the universal gas constant (8.314J/mol K). ΔG (kJ/mol), ΔH (kJ/mol), enthalpy, and ΔS (J mol^{-1} K^{-1}), entropy, are changes of Gibbs free energy. Plotting $\ln(Q_e/C_e)$ against $1/T$ gives a straight line with slope and intercept equal to $-\Delta H/T$ and $\Delta S/R$, respectively.

As shown in Table 4, when the temperature was increased from 298 to 318 K, ΔG decreased from −3.3714 to −6.2020 kJ/mol, indicating that the adsorption is spontaneous and higher temperature is more conductive to the adsorption process. Furthermore, the positive value of ΔH shows that the adsorption process is endothermic in nature.

Table 4. Thermodynamic Parameters for Ametryn onto CGC

T (K)	ΔG^0 (kJ mol^{-1})	ΔH^0 (kJ mol^{-1})	ΔS^0 (J mol^{-1} K^{-1})
288	−3.3714	20.0534	72.6444
298	−4.9180		
308	−6.2020		

According to the adsorption theory, for solid−liquid exchange adsorption, ametryn as a solute molecule would lose a part of the free degree (including translation and rotation) by exchanging from liquid phase to solid phase, which is the process of decreasing entropy.[47] However, a lot of water is desorpted at the same time. That is the process of increasing entropy. Because water has a small volume, entropy in value is larger than the former. These two parts contributed to total entropy variables, namely, that the total entropy variable is a positive value, indicating that adsorption for ametryn onto CGC is the process of increasing entropy.

To a certain extent, the type of adsorption can be distinguished from the magnitude of the enthalpy variable. If the binding energy is less than 84 kJ/mol, it can be considered as physical adsorption generally, while the binding energy of chemical adsorption is usually 84−420 kJ/mol.[39] According to Table 4, the enthalpy variable is 20.0534 kJ/mol, indicating adsorption of the CGC is a physical adsorption process. This conclusion is similar to the previous reports.[48]

Regeneration and Reuse of CGC. Desorption studies for the CGC can provide useful information for adsorption mechanism and commercial applications. Because triazine pesticides can be well dissolved in acetonitrile, desorption experiments were performed using acetonitrile. The desorption percentage of acetonitrile is no less than 95%, indicating that the CGC could be recycled by some simple organic solvent.

The results of six consecutive adsorptions and desorptions are shown in Figure 13. The adsorption efficiency of the CGC for ametryn was still over 85% after the sixth cycle. The results proved that CGC was a stable and effective adsorbent for triazine pesticides.

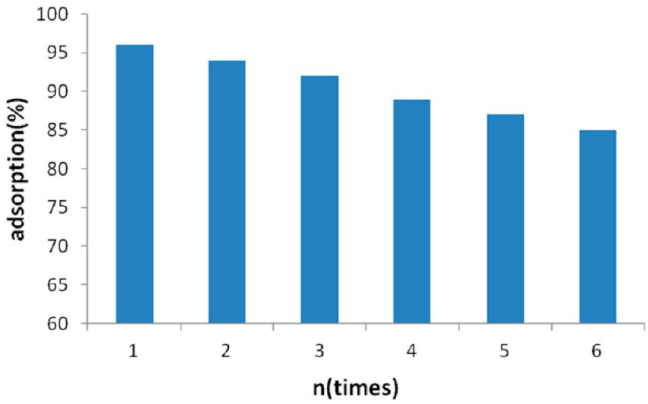

Figure 13. Regenerative functions of CGC.

CONCLUSIONS

The CGC has been prepared as a highly efficient sorbent, whose ability to adsorb six triazine pesticides is tested. The synthesis comprises a straightforward reduction of GO to modify the cellulose. The material is fully characterized using Fourier transform infrared spectroscopy, XRD, Raman spectroscopy, XPS, SEM, TEM, and elemental analyses. The results prove that the cellulose is successfully modified by the RGO. As active adsorption sites, the rough and wrinkled surfaces with a lamellar structure in the composite provide an advantageous condition and remarkably improve the adsorption rate compared to that of graphite carbons, PSA, GCB, cellulose, and graphene. The adsorption process only requires adding 30 mg of CGC for 10 mL of solution of triazine pesticides. The tests on the adsorption isotherms reveal that the Langmuir model describes the adsorption process better. Adsorption is spontaneous, favorable, and endothermic in nature. According to thermodynamic parameters, adsorption is a physical adsorption process with increasing entropy. In addition, the adsorption efficiency of the CGC is still over 85% after six times of recycling using a simple organic solvent. Therefore, this investigation proves that the cellulose modified by RGO is an efficient and stable adsorbent for triazine pesticides in water. The potential adsorption capability of the cellulose deserves further investigation.

ASSOCIATED CONTENT

Supporting Information

Consistency of the absorption performance (%) of CGC, XPS survey scan spectra of CGC, and plot of $\ln(Q_e/C_e)$ against $1/T$. This material is available free of charge via the Internet at http://pubs.acs.org.

AUTHOR INFORMATION

Corresponding Authors

*Tel: (+86)-10-6273-3620. E-mail: mayongqiang@cau.edu.cn (Y.M.).

*Tel: (+86)-10-80799135. E-mail: yanlidu@126.com (Y.D.).

Notes

The authors declare no competing financial interest.

DOI: 10.1021/sc500738k
ACS Sustainable Chem. Eng. 2015, 3, 396−405

■ ACKNOWLEDGMENTS

The authors thank the following organizations for support of this project: National Science Foundation for Fostering Talents in Basic Research of China (J1210064), Instrumentation special project (2013YQ510391) from the Chinese Ministry of Science and Technology, and Science and Technology Fund of Beijing Municipal Commission of Education (KZ201210020019).

■ REFERENCES

(1) Cacho, C.; Turiel, E.; Martin-Esteban, A. Clean-up of triazines in vegetable extracts by molecularly-imprinted solid-phase extraction using a propazine-imprinted polymer. *Anal. Bioanal. Chem.* **2003**, *376*, 491−496.

(2) Peng, L.; Xin, Y.; Hong, M.; Zhao, Y. F.; Liu, W.; Wu, Y. N. Simultaneous determination of 19 triazine pesticides and degradation products in processed cereal samples from Chinese total diet study by isotope dilution−high performance liquid chromatography−linear ion trap mass spectrometry. *Anal. Chim. Acta* **2013**, *781*, 63−71.

(3) Stepan, R.; Ticha, J.; Hajslova, J.; Kovalczuk, T.; Kocourek, V. Baby food production chain: Pesticide residues in fresh apples and products. *Food Addit. Contam.* **2005**, *22*, 1231−1242.

(4) Lykins, B.; Koffskey, W.; Miller, R. Chemical products and toxicological effects of disinfection. *J. Am. Water Works Assoc.* **1986**, *78*, 66−75.

(5) Miltner, R. J.; Baker, D. B.; Speth, T. F.; Fronk, C. A. Treatment of seasonal pesticides in surface waters. *J. Am. Water Works Assoc.* **1989**, *81*, 43−52.

(6) Jiang, H.; Adams, C. Treatability of chloro-s-triazines by conventional drinking water treatment technologies. *Water Res.* **2006**, *40*, 1657−1667.

(7) Ormad, M. P.; Miguel, N.; Claver, A.; Matesanz, J. M.; Ovelleiro, J. L. Pesticides removal in the process of drinking water production. *Chemosphere.* **2008**, *71*, 97−106.

(8) Plakas, K. V.; Karabelas, A. J. Removal of pesticides from water by NF and RO membranes − A review. *Desalination.* **2012**, *287*, 255−265.

(9) Boussahel, R.; Bouland, S.; Moussaoui, K. M.; Montiel, A. Removal of pesticide residues in water using the nanofiltration process. *Desalination* **2000**, *132*, 205−209.

(10) Reynolds, G.; Graham, N.; Perry, R.; Rice, R. G. Aqueous ozonation of pesticides: A review. *Ozone Sci. Eng.* **1989**, *11*, 339−382.

(11) Lai, M. S.; Jensen, J. N.; Weber, A. S. Oxidation of simazine: Ozone, ultraviolet, and combined ozone/ultraviolet oxidation. *Water Environ. Res.* **1995**, *67*, 340−346.

(12) Siro, I.; Plackett, D. Microfibrillated cellulose and new nanocomposite materials: A review. *Cellulose.* **2010**, *17*, 459−494.

(13) Zhang, X.; Liu, X.; Zheng, W. Regenerated cellulose/graphene nanocomposite films prepared in DMAC/LiCl solution. *Carbohydr. Polym.* **2012**, *88*, 26−30.

(14) Sen, S.; Martin, J. D.; Argyropoulos, D. S. Review of cellulose non-derivatizing solvent interactions with emphasis on activity in inorganic molten salt hydrates. *ACS Sustainable Chem. Eng.* **2013**, *1*, 858−870.

(15) Shi, X.; Zhang, L.; Cai, J. A facile construction of supramolecular complex from polyaniline and cellulose in aqueous system. *Macromolecules* **2011**, *44*, 4565−4568.

(16) Balog, R.; Jorgensen, B.; Nilsson, L.; Andersen, M.; Rienks, E.; Bianchi, M. Bandgap opening in graphene induced by patterned hydrogen adsorption. *Nat. Mater.* **2010**, *9*, 315−319.

(17) Liu, X. T.; Zhang, H. Y.; Ma, Y. Q.; Wu, X. L.; Meng, L. X.; Guo, Y. L.; Yu, G.; Liu, Y. Q. Graphene-coated silica as a highly efficient sorbent for residual organophosphorus pesticides in water. *J. Mater. Chem. A* **2013**, *1*, 1875−1884.

(18) Feng, Y. Y.; Zhang, X. Q.; Shen, Y. T.; Katsumi, Y.; Feng, W. A mechanically strong, flexible and conductive film based on bacterial cellulose/graphene nanocomposite. *Carbohydr. Polym.* **2012**, *87*, 644−649.

(19) Weng, Z.; Su, Y.; Wang, D. W.; Li, F.; Du, J. H.; Cheng, H. M. Graphene−cellulose paper flexible supercapacitors. *Adv. Energy Mater.* **2011**, *1*, 917−922.

(20) Shi, H. C.; Li, W. S.; Zhong, Lei. Methylene blue adsorption from aqueous solution by magnetic cellulose/graphene oxide composite: equilibrium, kinetics, and thermodynamics. *Eng. Chem. Res.* **2014**, *53*, 1108−1118.

(21) Offeman, R. E.; Hummers, W. S. Preparation of graphitic oxide. *J. Am. Chem. Soc.* **1958**, *80*, 1339−1339.

(22) Gao, K.; Shao, Z.; Wu, X.; Wang, X.; Li, J.; Zhang, Y.; Wang, F. Cellulose nanofibers/reduced graphene oxide flexible transparent conductive paper. *Carbohydr. Polym.* **2013**, *97*, 243−251.

(23) Tian, M.; Qu, L.; Zhang, X.; Zhang, K.; Zhu, S.; Guo, X.; Sun, Y. Enhanced mechanical and thermal properties of regenerated cellulose/graphene composite fibers. *Carbohydr. Polym.* **2014**, *111*, 456−462.

(24) Vimlesh, C.; Jaesung, P.; Young, C.; Jung, W. L. Water-dispersible magnetite-reduced graphene oxide composites for Arsenic removal. *ACS NANO.* **2010**, *7*, 3979−3986.

(25) Zhang, K.; Zhang, L. L.; Zhao, X. S.; Wu, J. S. Graphene/polyaniline nanofiber composites as supercapacitor electrode. *Chem. Mater.* **2010**, *22*, 1392−1401.

(26) Gao, K.; Shao, Z.; Li, J.; Wang, X.; Peng, X.; Wang, W.; Wang, F. Cellulose nanofiber−graphene all solid-state flexible supercapacitors. *J. Mater. Chem. A* **2013**, *1*, 63−67.

(27) Ciolacu, D.; Ciolacu, F.; Popa, V. I. Amorphous cellulose-structure and characterization. *Cellul. Chem. Technol.* **2011**, *45*, 13.

(28) Carrasco, P. M.; Montes, S.; Garcia, I.; Borghei, M.; Jiang, H.; Odriozola, I.; Ruiz, V. High-concentration aqueous dispersions of graphene produced by exfoliation of graphite using cellulose nanocrystals. *Carbon.* **2014**, *70*, 157−163.

(29) Chandra, V.; Kim, K. S. Highly selective adsorption of Hg^{2+} by a polypyrrole-reduced graphene oxide composite. *Chem. Commun.* **2011**, *47*, 3942−3944.

(30) Boukhvalov, D. W.; Katsnelson, M. I. Modeling of graphite oxide. *J. Am. Chem. Soc.* **2008**, *130*, 10697−10701.

(31) Yang, Q.; Pan, X. J.; Li, K. C. Covalent functionalization of graphene with polysaccharides. *Eng. Chem. Res.* **2012**, *51*, 310−317.

(32) Zhao, H. B.; Kwak, J. H.; Conrad Zhang, Z. Studying cellulose fiber structure by SEM, XRD, NMR and acid hydrolysis. *Carbohydr. Polym.* **2007**, *68*, 235−241.

(33) Wang, J.; Tsuzuki, T.; Tang, B. Reduced graphene oxide/ZnO composite: Reusable adsorbent for pollutant management. *ACS Appl. Mater. Interfaces.* **2012**, *4*, 3084−3090.

(34) Ouyang, W.; Sun, J.; Memon, J.; Wang, C.; Geng, J.; Huang, Y. Scalable preparation of three-dimensional porous structures of reduced graphene oxide/cellulose composites and their application in supercapacitors. *Carbon.* **2013**, *62*, 501−509.

(35) Zhang, X.; Liu, X.; Zheng, W.; Zhu, J. Regenerated cellulose/graphene nanocomposite films prepared in DMAC/LiCl solution. *Carbohydr. Polym.* **2012**, *88*, 26−30.

(36) Jannik, C. M.; Geim, A. K.; Katsnelson, M. I.; Novoselov, K. S.; Booth, T. J.; Roth, S. The structure of suspended graphene sheets. *Nat. Lett.* **2007**, *446*, 60−63.

(37) Guoxiu, W.; Juan, Y.; Jinsoo, P.; Xinglong, G.; Bei, W.; Hao, L.; Jane, Y. Facile synthesis and characterization of graphene nanosheets. *J. Phys. Chem. C* **2008**, *112*, 8192−8195.

(38) Guoxiu, W.; Bei, W.; Jinsoo, P.; Juan, Y.; Xiaoping, S.; Jane, Y. Synthesis of enhanced hydrophilic and hydrophobic graphene oxide nanosheets by a solvothermal method. *Carbon.* **2009**, *47*, 68−72.

(39) Xiong, Z. H.; Wang, L.; Zhou, J. G. Thermodynamics, thermochemistry and solution chemistry. *Acta Phys. Chim. Sin.* **2010**, *26*, 2890−2898.

(40) Ramesha, G. K.; Vijaya Kumara, A.; Muralidhara, H. B.; Sampath, S. Graphene and graphene oxide as effective adsorbents toward anionic and cationic dyes. *J. Colloid Interface Sci.* **2011**, *361*, 270−277.

(41) Hu, S. W.; Chen, S. Adsorption of triazine derivatives with humic fraction-immobilized silica gel in hexane: A mechanistic consideration. *J. Agric. Food. Chem.* **2013**, *61*, 8524−8532.

DOI: 10.1021/sc500738k
ACS Sustainable Chem. Eng. 2015, 3, 396−405

(42) Leenaerts, O.; Partoens, B.; Peeters, F. M. Adsorption of small molecules on graphene. *Microelectron. J.* **2009**, *40*, 860−862.
(43) Bermudez, V. M.; Robinson, J. T. Effects of molecular adsorption on the electronic structure of single-layer graphene. *Langmuir.* **2011**, *27*, 11026−11036.
(44) Pirkle, W. H.; Pochapsky, T. C.; Mahler, G. S.; Field, R. E. Chromatographic separation of the enantiomers of 2-carboalkoxyindolines and N-aryl-α-amino esters on chiral stationary phases derived from N-(3, 5-dinitrobenzoyl)-α-amino acids. *J. Chromatogr. A* **1985**, *348*, 89−96.
(45) Guo, S.; Liang, S.; Feng, N.; Tian, Q. Isotherms, kinetics and thermodynamic studies of adsorption of Cu2+ from aqueous solutions by Mg^{2+}/K^{+} type orange peel adsorbents. *J. Hazard. Mater.* **2010**, *174*, 756−762.
(46) Neghlani, P. K.; Rafizadeh, M.; Taromi, F. A. Preparation of aminated-polyacrylonitrile nanofiber membranes for the adsorption of metal ions: Comparison with microfibers. *J. Hazard. Mater.* **2011**, *186*, 182−189.
(47) Werner, H. J.; Schütz, M. An efficient local coupled cluster method for accurate thermochemistry of large systems. *J. Chem. Phys.* **2011**. http://dx.doi.org/10.1063/1.3641642 (accessed August 31, 2011).
(48) Mittendorfer, F.; Garhofer, A.; Redinger, J.; Klimes, J.; Harl, J.; Kresse, G. Graphene on Ni (111): Strong interaction and weak adsorption. *Phys. Rev. B* **2011**, *84*, 201401.

DOI: 10.1021/sc500738k
ACS Sustainable Chem. Eng. 2015, 3, 396−405